PROTEINS
STRUCTURE ■ FUNCTION ■ BIOINFORMATICS

STRUCTURE NOTE

Structure of the C-terminal domain of *Saccharomyces cerevisiae* Nup133, a component of the nuclear pore complex

Parthasarathy Sampathkumar,[1]* Tarun Gheyi,[1] Stacy A. Miller,[1] Kevin T. Bain,[1] Mark Dickey,[1] Jeffrey B. Bonanno,[2] Seung Joong Kim,[3,4,5] Jeremy Phillips,[3,4,5,6] Ursula Pieper,[3,4,5] Javier Fernandez-Martinez,[7] Josef D. Franke,[7] Anne Martel,[8] Hiro Tsuruta,[8] Shane Atwell,[1] Devon A. Thompson,[1] J. Spencer Emtage,[1] Stephen R. Wasserman,[9] Michael P. Rout,[7] Andrej Sali,[3,4,5] J. Michael Sauder,[1] and Stephen K. Burley[1]

[1] New York SGX Research Center for Structural Genomics, (NYSGXRC), Eli Lilly and Company, Lilly Biotechnology Center, San Diego, California 92121

[2] Department of Biochemistry, Albert Einstein College of Medicine, Bronx, New York 10461

[3] Department of Bioengineering and Therapeutic Sciences, University of California, San Francisco, California 94158

[4] Department of Pharmaceutical Chemistry, University of California, San Francisco, California 94158

[5] California Institute for Quantitative Biosciences, University of California, San Francisco, California 94158

[6] Graduate Group in Biological and Medical Informatics, University of California, San Francisco, California 94158

[7] Laboratory of Cellular and Structural Biology, The Rockefeller University, New York, New York 10065

[8] Stanford Synchrotron Radiation Lightsource, Stanford Linear Accelerator Center, MS 69, Menlo Park, California 94025-7015

[9] LRL-CAT, Eli Lilly and Company, Advanced Photon Source, Argonne National Laboratory, Illinois 60439

Key words: nuclear pore complex; Nup133; structural genomics.

INTRODUCTION

Nuclear pore complexes (NPCs) are situated at the interface of the inner and outer nuclear membranes, where they are responsible for transport of biomolecules between nucleus and cytoplasm of eukaryotic cells.[1–3] *Saccharomyces cerevisiae* NPCs are ~50 MDa assemblies made up of at least 456 polypeptides of ~30 different sequences, called nucleoporins or Nups.[4,5] Several of these Nups, sharing similar structural motifs, assemble into stable subcomplexes that are arranged with eightfold symmetry to form a co-axial ring structure containing a membrane ring, two outer (nuclear and cytoplasmic) rings and two inner rings. One of these subcomplexes in the yeast NPC is the Nup84 complex that is situated within the nuclear and cytoplasmic peripheral rings.[5] The Nup84 complex is a heptameric assembly forming a Y-shaped structure composed of Nup84, Nup85, Nup120, Nup133, Nup145C, Sec13, and Seh1.[6] The homologous metazoan complex is a nonameric assembly termed the Nup107–160 complex, carrying homologues of all seven yeast Nups plus Nup37 and Nup43 as additional components.[7] Nup133 is a ~1150 residue protein containing an N-terminal seven blade β-propeller domain followed by an ~80 kDa helical domain.[8–10] The C-terminal domain

Grant sponsor: NIH; Grant number: U54 GM074945, R01 GM062427, NIH R01 GM083960, and NIH U54 RR022220; Grant sponsor: U. S. Department of Energy, Office of Science, Office of Basic Energy Sciences; Grant number: DE-AC02-06CH11357; Grant sponsor: Office of Science, Office of Biological and Environmental Research, U.S. Department of Energy; Grant number: DE-AC02-05CH11231

*Correspondence to: Parthasarathy Sampathkumar, Lilly Biotechnology Center, 10300 Campus Point Drive, Suite 200, San Diego, CA 92121, USA.
E-mail: spartha2@gmail.com; sampathkumarpa@lilly.com

Received 5 August 2010; Revised 16 November 2010; Accepted 23 November 2010
Published online 4 January 2011 in Wiley Online Library (wileyonlinelibrary.com).
DOI: 10.1002/prot.22973

of human Nup133, in particular, residues 934–1156 [HsNup133(934–1156)], is essential for its binding to Nup107, together forming the stem of the Y-shaped complex. Crystal structures of the HsNup133(934–1156) have been determined in complex with Nup107 (residues 658–925). In this complex, 11 HsNup133(934–1156) helices are arranged as two helical blocks.[11,12]

We have determined the structure of the *S. cerevisiae* Nup133 (ScNup133) C-terminal helical domain at 1.9 Å resolution, corresponding to residues 944–1157 [ScNup133(944–1157)]. Our structure reveals a compact helical arrangement, differing in several respects from the structure of the homologous HsNup133(934–1156) determined in complex with Nup107. We also report small-angle X-ray scattering (SAXS) of ScNup133(944–1157) in solution that is consistent with our compact crystallographically observed structure.

EXPERIMENTAL

Cloning, expression, and purification of ScNup133(944–1157)

ScNup133 comprising residues 881–1157 was cloned from the genomic DNA of the yeast strain Sc2601D-5 (American Type Culture Collection, USA). The desired construct was PCR amplified using the forward, AAG TACGGTCATGTAGCATGGA and, reverse, CGTATTCTA CAGTGTTGGTTTCATAG, primers and subsequently TOPO® (Invitrogen, USA) cloned into pSGX3, a derivative of pET26 b(+), giving rise to proteins with a noncleavable C-terminal hexa histidine tag. Plasmids were transformed into BL21 (DE3)-Condon + RIL (Invitrogen) cells for overexpression. Expression of selenomethionine-labeled proteins was carried out in 3 L of HY media at 22°C with 50 μg/mL of kanamycin and 35 μg/mL of chloramphenicol. Protein expression was induced at $O.D._{600}$ ~1.0 by addition of 0.4 m*M* IPTG. Cells were harvested after 21 h by centrifugation at 4°C.

For purification, the *E. coli* cell pellet was resuspended in 30 mL of cold buffer containing 20 m*M* Tris–HCl pH 8.0, 500 m*M* NaCl, 25 m*M* imidazole, and 0.1% Tween20 and cells were lysed by sonication. Debris was removed by centrifugation at 4°C. The decanted supernatant was applied to a 5-mL HisTrapHP column (GE Health Care, USA) charged with nickel and pre-equilibrated with 20 m*M* Tris–HCl pH 8.0, 500 m*M* NaCl, 10% v/v glycerol, and 25 m*M* imidazole. The sample was washed with five column volumes (CVs) of 20 m*M* Tris–HCl pH 8.0, 500 m*M* NaCl, 10% (v/v) glycerol, and 40 m*M* imidazole and subsequently eluted with 2 CV of same buffer with an imidazole concentration of 250 m*M*. Eluted protein was passed over a 120-mL Superdex 200 column equilibrated with 10 m*M* HEPES pH 7.5, 150 m*M* NaCl, 10% (v/v) glycerol, and 5 m*M* DTT (protein storage buffer). SDS–PAGE analysis showed greater than 95% purity, and protein fractions corresponding to the symmetric portion of the size exclusion chromatography profile were pooled for concentration using AMICON spin filters. Concentrated protein aliquots were frozen in liquid nitrogen and stored at −80°C.

Crystallization, data collection, and structure determination

ScNup133(944–1157), at a concentration of 17.6 mg/mL, was subjected to crystallization screening with the Classics, Classics II, and PEGs kits (Qiagen, USA) using a Phoenix Liquid Handling Systems (Art Robins, USA) with equal volumes (0.3 μL) and reservoir solution in 96-well sitting drop format at 21°C. Diffracting quality crystals were obtained with 20% PEG3350 in the presence of 200 m*M* potassium thiocyanate (PEGs suite; condition number 62) and were cryoprotected with the addition of ~30% (v/v) glycerol before being flash frozen by immersion in liquid nitrogen. Diffraction data were recorded using the LRL-CAT 31-ID beamline at the advanced photon source (APS) and processed with MOSFLM[13] and SCALA (Collaborative Computing Project Number 4, 1994).[14] About 800 reflections were randomly selected for cross validation representing an *R*-free dataset. The structure of ScNup133(944–1157) was determined by the single-wavelength anomalous dispersion method, using data collected at a wavelength of 0.97929 Å, corresponding to the "Se peak" absorption edge. A single Se atom was located with SHELXD,[15] and phases were calculated using SHELXE as implemented in HKL2MAP.[16] Following numerous rounds of automated and manual model building with ARP/wARP[17] and COOT,[18] respectively, the atomic coordinates were refined using REFMAC5[19] as implemented in CCP4. The polypeptide backbone of ScNup133 could be traced continuously from residue Lys946 to Tyr1157 in the electron density maps. The final refined atomic model of ScNup133(944–1157) has excellent stereochemistry (Table I). Structural analyses were carried out using COOT and CCP4, and illustrations were prepared using PyMol (http://pymol.sourceforge.net).

Small-angle X-ray scattering

Small-angle X-ray scattering (SAXS) measurements of ScNup133(944–1157) were carried out on the SIBYLS Beamline 12.3.1 at the advanced light source (ALS), Lawrence Berkeley National Laboratory. Samples were prepared on a 96-well plate and kept at 10°C until SAXS measurement. An automatic sample delivery system equipped with a Hamilton pipetting robot was used.[22] SAXS data were collected on a MAR165 area detector (Rayonix), placed at 1.5 m from the SAXS sample cell. Exposures of 2 sec/10 sec/2 sec were made in series for each protein sample maintained at 10°C. Each of the diffraction images was scaled using the transmitted beam intensity, azimuthally

Table I
Crystallographic Statistics

Data collection	ScNup133(944–1157)
PDB code	3KFO
Space group	$P2_12_12_1$
Unit-cell dimensions *a*, *b*, and *c* (Å)	*a* = 47.4, *b* = 52.7, *c* = 76.7
Matthew's coefficient (Å^3/Da)	1.89
Solvent content (%)	34.45
Resolution (Å)	31.00–1.90 (2.00–1.90)*
Number of unique reflections	15,683
Completeness (%)	99.7 (100.0)
R_{symm} (%)	12.1 (41.4)
Multiplicity	7.7 (7.8)
$<I/\sigma(I)>$	10.6 (4.6)
Refinement	
R_{cryst} (%)	19.1
R_{free} (%)	24.8
RMS deviations from ideal values	
Bond length (Å)	0.019
Bond angles (°)	1.63
Average B-factors (Å^2)	
Protein	23.4
Water molecules	31.5
Cosolvent (glycerol)	45.7
Ramachandran Plot[20]	
MolProbity[21] residues in favored region (%)	99.5
Allowed region (%)	100.0

[a]Values in parenthesis correspond to the highest-resolution shell.

integrated, and averaged to obtain fully processed data in the form of intensity versus q [$q = 4\pi \sin(\theta)/\lambda$, θ = one-half of the scattering angle; λ = X-ray wavelength]. The buffer profile was obtained in the same manner and subtracted from a protein profile. SAXS profiles of ScNup133(944–1157) were recorded at protein concentrations of 0.5, 1.0, 2.0, 5.0, and 17.6 mg/mL in protein storage buffer. Moreover, mild concentration dependence was removed by extrapolating to zero concentration. We merged the average of the low-scattering angle parts ($q < 0.15$ Å^{-1}) of the low concentration profiles (0.5–2.0 mg/mL) and the average of the high-scattering angle parts ($q > 0.12$ Å^{-1}) of the high concentration (5.0–17.6 mg/mL) profiles to obtain the final, merged experimental SAXS profile. SAXS profiles were calculated with IMP-FoXS[23,24] (http://salilab.org/foxs/) and CRYSOL[25] and compared to the merged experimental SAXS profile. A complete structural model of ScNup133(944–1157), including two N-terminal residues (Leu-Arg), C-terminal hexa-histidine tag (Gly-His-His-His-His-His-His), and 16 missing side chains, was generated using its crystal structure with the automatic PSF-based model building option of VMD[26] and the automodel function of MODELLER[27] (these missing atoms were not included in the final X-ray structure, because they appear disordered in the electron density map). Inclusion of the missing atoms improved the fit of the calculated SAXS profiles to our experimental observations (χ^2 value improved from 2.95 to 1.25), particularly at higher scattering angles ($q > 0.2$ Å^{-1}). The shape of ScNup133(944–1157) was calculated from the merged experimental SAXS profile by running DAMMIF[28] and GASBOR[29] 20 times individually, followed by superposition and averaging with DAMAVER.[30]

RESULTS AND DISCUSSION

Structure of ScNup133(944–1157)

The expected molecular weight of ScNup133 (residues 881–1157) is 33,025 Da. The measured molecular weight, using mass spectrometry, of the final purified selenomethionine form of ScNup133 was 25,871 Da (mass error < 0.007%). The difference in mass of −7154 Da was attributed to unintended N-terminal proteolysis during expression and/or purification (the presence of an intact C-terminus with hexa-histidine affinity tag was confirmed by binding the purified ScNup133 to Ni-NTA resin). N-terminal sequencing documented that the truncation occurred at the Thr943-Leu944 peptide bond. The resulting target protein, consisting of residues 944–1157 [ScNup133(944–1157)], yielded crystals diffracting to 1.9 Å resolution (orthorhombic $P2_12_12_1$ space group, one molecule per asymmetric unit, Table I). Electron density maps phased with a single selenium atom allowed continuous tracing of the ScNup133 polypeptide backbone from Lys946 to Tyr1157.

The overall fold of ScNup133(944–1157) is composed of 11 α-helices with a short two-stranded β-sheet, formed by β2–β3, at the C-terminus [Fig. 1(A)]. Helices α1–α11 form a compact structure. A four helical bundle (formed by the α3, α4, α5, and α6 helices) at the center of the structure is surrounded by the α1, α2, α9, α10, and α11 helices. A search for structurally similar proteins using DALI[34] did not identify any known structures with *Z*-scores > 10. Highest *Z*-scores of 5.0 were obtained for PDB (http://www.rcsb.org) codes 3IHV and 3DWL, which correspond to a sugar-binding protein SusD homolog (sequence identity = 8%; root mean square deviation = 3.6 Å for 112 C^α atomic pairs) and subunit 5 of the actin-related protein 2/3 complex (sequence identity = 12%; r.m.s.d. = 3.4 Å for 95 C^α atomic pairs), respectively. It is likely that the structural similarities of these two proteins to ScNup133(944–1157) are due to geometrical restraints on the packing of helices rather than to a common ancestor in evolution. The absence of the human Nup133 structure among the top scoring DALI hits came as a surprise, prompting us to measure the SAXS profile of ScNup133(944–1157) to determine whether or not the arrangement of helices observed in our crystal structure is an artifact of crystallization.

The merged experimental SAXS profile closely resembles the SAXS profile calculated from the complete model of ScNup133(944–1157) obtained with the X-ray structure of [Fig. 1(B)]. The measured radius of gyration (R_g) of 18.8 ± 0.5 Å, obtained from AutoRg,[35] compares within the experimental errors with the R_g of 18.6 Å for

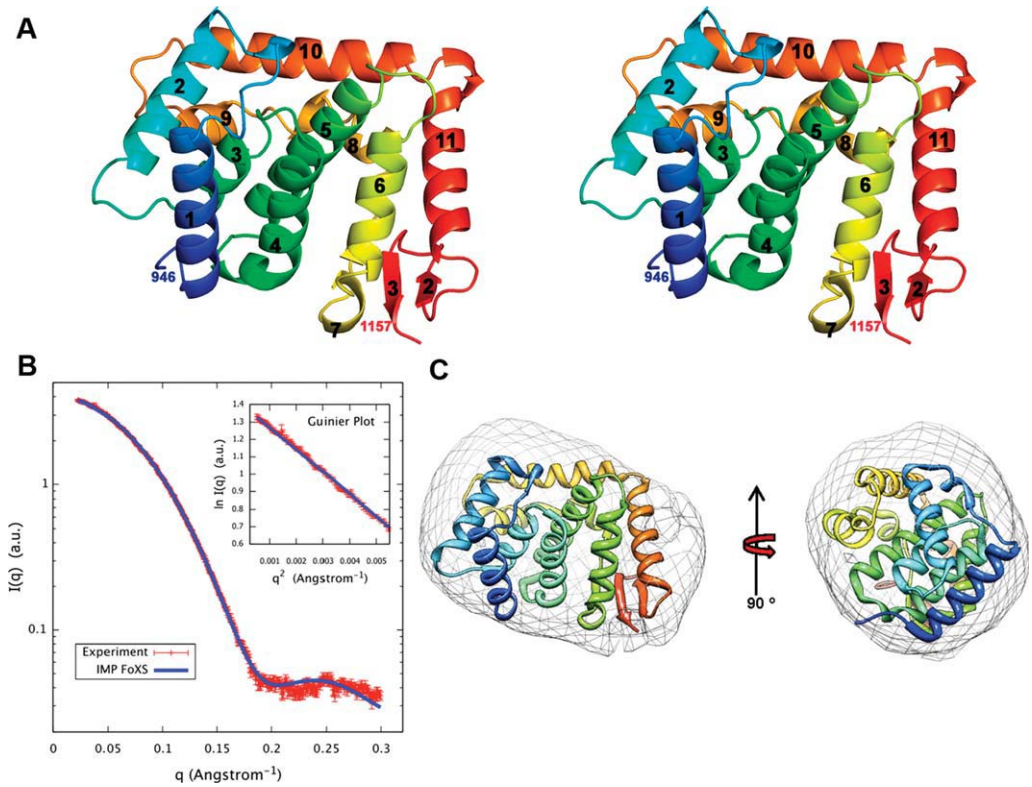

Figure 1

A: Stereo view of a ribbon representation of ScNup133(944–1157). Secondary structure elements were assigned by DSSP.[31] The fold is colored blue to red from the N- to C-termini. **B**: Comparison of the merged experimental SAXS profile (red) of ScNup133(944–1157) with SAXS profiles computed by IMP-FoXS[32,33] (blue) for the complete model of ScNup133(944–1157). Inset shows the SAXS profiles in the Guinier plot. D_{max} of radial distribution function, $P(r)$ is 56.25 Å. **C**: The shape of ScNup133(944–1157) derived from the experimental SAXS profile, shown in two orthogonal orientations.

the crystal structure and R_g of 19.3 Å for the complete model. The ab initio shape reconstructed from the merged experimental SAXS profile with DAMMIF[28] [Fig 1(C)] and GASBOR[29] (not shown) matches the overall structure of ScNup133(944–1157). Therefore, SAXS analysis indicates that the compact fold of ScNup133

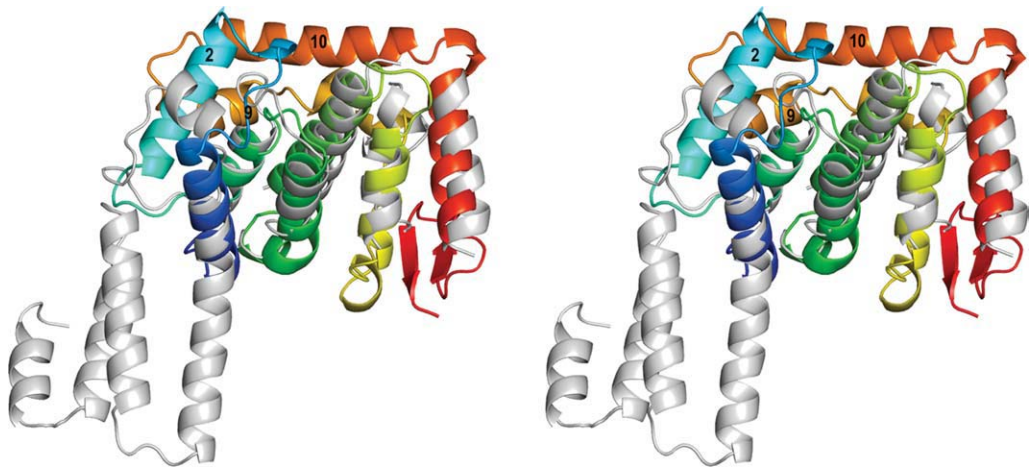

Figure 2

A: Structural superposition of the C-terminal domains of Sc and Hs Nup133. ScNup133(944–1157) is shown as in Figure 1(A) and HuNup133(934–1156) is shown in gray.

(944–1157) exists in solution and is not an artifact of crystallization.

Comparison of ScNup133(944–1157) with human Nup133

Structures of human Nup133 residues 934–1156 [HsNup133(934–1156)] have only been determined in complexes with Nup107 (PDB Codes 3CQC,[10] 3CQG,[10] and 3I4R[11]). The amino acid sequence identity between the C-terminal domains of Sc and Hs Nup133 is rather low, ~12%. Structure-based alignments did not yield complete coverage of the two polypeptide chains. Structure-based alignment using Multiprot[35] resulted in a r.m.s.d. of 1.6 Å for 88 C^{α} atomic pairs with sequence identity of ~9%. The r.m.s.d. for structure-based alignment using SSM[32] is 2.5 Å for 98 C^{α} atomic pairs with sequence identity of ~8%. In the case of ScNup133, we have lost the putative Nup84 interaction surface due to the proteolysis. Therefore, the first helix α1 of ScNup133 aligns with the α4 of the HsNup133 structure [Fig. 2]. The four helical bundle present at the center of both ScNup133(944–1157) and HuNup133(934–1156) superpose well over each other along with the α11 helix. However, HsNup133(934–1156) lacks counterparts to ScNup133(944–1157) helices α2, α9, and α10; and β-strands. Therefore, two homologous Nups from two distantly related organisms show significant sequence and structural divergence in their C-termini. These differences show that a single example structure from each Nup obtained from just one organism does not represent the range of structures present throughout the Eukaryota among different Nups in different states. Thus, there is a pressing need for more structures of NPC components, from various organisms, both alone and in complexes with their respective binding partners.

ACKNOWLEDGMENTS

We thank members of the Rout and Sali laboratories for their help and advice, in particular Dina Schneidmann for help with the IMP-FoXS SAXS web server. We are also grateful to Drs. John Tainer and Michal Hammel for help in using the SIBYLS beamline 12.3.1 at ALS. Use of the Lilly Research Laboratories Collaborative Access Team (LRL-CAT) beamline at Sector 31 of the APS was provided by Eli Lilly and Company, which operates the facility. Protein data bank codes: Coordinates and structure factors of ScNup133(944–1157) were deposited to the PDB on October 27, 2009 with accession code 3KFO. The NYSGXRC target identifier for yeast Nup133 is TargetDB (http://targetdb.pdb.org), "NYSGXRC-15133a." Clone sequences and experimental information are available in PepcDB (http://pepcdb.pdb.org/).

REFERENCES

1. Rout MP, Aitchison JD, Suprapto A, Hjertaas K, Zhao YM, Chait BT. The yeast nuclear pore complex: composition, architecture, and transport mechanism. J Cell Biol 2000;148:635–651.
2. D'Angelo MA, Hetzer MW. Structure, dynamics and function of nuclear pore complexes. Trends Cell Biol 2008;18:456–466.
3. Elizabeth JT, Wente SR. Dynamic nuclear pore complexes: life on the edge. Cell 2006;125:1041–1053.
4. Alber F, Dokudovskaya S, Veenhoff LM, Zhang WH, Kipper J, Devos D, Suprapto A, Karni-Schmidt O, Williams R, Chait BT, Sali A, Rout MP. The molecular architecture of the nuclear pore complex. Nature 2007;450:695–701.
5. Alber F, Dokudovskaya S, Veenhoff LM, Zhang WZ, Kipper J, Devos D, Suprapto A, Karni-Schmidt O, Williams R, Chait BT, Rout MP, Sali A. Determining the architectures of macromolecular assemblies. Nature 2007;450:683–694.
6. Lutzmann M, Kunze R, Buerer A, Aebi U, Hurt E. Modular assembly of a Y-shaped multiprotein complex from seven nucleoporins. EMBO J 2002;21:387–397.
7. Loiodice I, Alves A, Rabut G, Van Overbeek M, Ellenberg J, Sibarita JB, Doye V. The entire Nup107–160 complex, including three new members, is targeted as one entity to kinetochores in mitosis. Mol Biol Cell 2004;15:3333–3344.
8. Doye V, Wepf R, Hurt EC. A novel nuclear pore protein Nup133p with distinct roles in poly(A)+ RNA transport and nuclear pore distribution. EMBO J 2002;21:387–397.
9. Pemberton LF, Rout MP, Blobel G. Disruption of the nucleoporin gene NUP133 results in clustering of nuclear pore complexes. Proc Natl Acad Sci USA 92;1187–1191.
10. Berke IC, Boehmer T, Blobel G, Schwartz TU. Structural and functional analysis of Nup133 domains reveals modeular building blocks of the nuclear pore complex. J Cell Biol 2004;22:591–597.
11. Boehmer T, Jeudy S, Berke IC, Schwartz TU. Structural and functional studies of Nup107/Nup133 interaction and its implications for the architecture of the nuclear pore complex. Mol Cell 2008;30:721–731.
12. Whittle JRR, Schwartz TU. Architectural nucleoporins Nup157/170 and Nup133 are structurally related and discend from a second ancestral element. J Biol Chem 2009;284:28442–28452.
13. Leslie AGW, Brick P, Wonacott AJ. An improved program package for the measurement of oscillation photographs. CCP4 News 1986;18:33–39.
14. Collaborative Computing Project Number 4. The CCP4 suite: programs for protein crystallography. Acta Crystallogr D Biol Crystallogr 1994;50:760–763.
15. Schneider TR, Sheldrick GM. Substructure solution with SHELXD. Acta Crystallogr D Biol Crystallogr 2002;58:1772–1779.
16. Pape T, Schneider TR. HKL2MAP: a graphical user interface for phasing with SHELX program. J Appl Cryst 2004;37:843–844.
17. Perrakis A, Morris R, Lamzin VS. Automated protein model building combined with iterative structure refinement. Nat Struct Biol 1999;6:458–463.
18. Emsley P, Cowtan K. COOT: model-building tools for molecular graphics. Acta Crystallogr D Biol Crystallogr 2004;60:2126–2132.
19. Murshudov GN, Vagin AA, Dodson EJ. Refinement of macromolecular structures by the maximum-likelihood method. Acta Crystallogr D Biol Crystallogr 1997;53:240–255.
20. Ramakrishnan C, Ramachandran GN. Stereochemical criteria for polypeptide and protein chain conformations. II. Allowed conformations for a pair of peptide units. Biophys J 1965;5:909–933.
21. Davis IW, Leaver-Fay A, Chen VB, Block JN, Kapral GJ, Wang X, Murray LW, Arendall WB, III, Snoeyink J, Richardson JS, Richardson DC Mol Probity: all-atom contacts and structure validation for proteins and nucleic acids. Nucl Acids Res 2007:35:W375–W383.
22. Hura GL, Menon AL, Hammel M, Rambo RP, Poole FL, II, Tsutakawa SE, Jenney FE, Jr, Classen S, Frankel KA, Hopkins RC, Yang S,

Scott JW, Dillard BD, Adams MWW, Tainer JA. Robust, high-throughput solution structural analyses by small angle X-ray scattering (SAXS). Nat Methods 2009;6:606–612.
23. Forster F, Webb B, Krukenberg KA, Tsuruta H, Agard DA, Sali A. Integration of small-angle X-ray scattering data into structural modeling of proteins and their assemblies. J Mol Biol 2008;382:1089–1106.
24. Schneidman-Duhovny D, Hammel M, Sali A. FoXS: a web server for rapid computation and fitting of SAXS profiles. Nucl Acids Res 2010;38 (Suppl):W540–W544.
25. Svergun DI, Barberato C, Koch MHJ. CRYSOL—a program to evaluate X-ray solution scattering of biological macromolecules from atomic coordinates. J Appl Cryst 1995;28:768–773.
26. Humphrey W, Dalke A, Schulten K. VMD—visual molecular dynamics. J Mol Graphics 1996;14:33–38.
27. Sali A, Blundell TL. Comparative protein modelling by satisfaction of spatial restraints. J Mol Biol 1993;234:779–815.
28. Franke D, Svergun DI. DAMMIF, a program for rapid ab-initio shape determination in small-angle scattering. J Appl Cryst 2009;42:342–346.
29. Svergun DI, Petoukhov MV, Koch MHJ. Determination of domain structure of proteins from X-ray solution scattering. Biophys J 2001;80:2946–2953.
30. Volkov VV, Svergun DI. Uniqueness of ab initio shape determination in small-angle scattering. J Appl Cryst 2003;36:860–864.
31. Kabsch W, Sander C. Dictionary of protein secondary structure: pattern recognition of hydrogen-bonded and geometrical features. Biopolymers 1983;22:1577–2637.
32. Shatsky M, Nussinov R, Wolfson HJ. A method for simultaneous alignment of multiple protein structures. Proteins Struct Funct Bioinform 2004;56:143–156.
33. Krissinel E, Henrick K. Secondary-structure matching (SSM), a new tool for fast protein structure alignment in three dimensions. Acta Crystallogr D Biol Crystallogr 2004;60:2256–2268.
34. Holm L, Kaariainen S, Rosenstrom P, Schenkel A. Searching protein structure database with DliLite v. 3. Bioinformatics 2008;24:2780–2781.
35. Konarev PV, Volkov VV, Sokolova AV, Koch MHJ, Svergun DI. PRIMUS: a Windows PC-based system for small-angle scattering data analysis. J Appl Cryst 2003;36:1277–1282.